# Explicit analytic formulas for Newtonian Taylor-Couette primary instabilities

C. S. Dutcher and S. J. Muller*

*Department of Chemical Engineering, University of California at Berkeley, Berkeley, California 94720, USA*

(Received 7 December 2006; published 3 April 2007)

In this study, existing primary stability boundary data for flow between concentric cylinders, for the broad range of radius and rotation ratios examined, were found to be self-similar in a properly chosen parameter space. The experimental results for the primary transitions to both Taylor vortex flow and spiral vortex flow collapsed onto a single curve using a combination of variables technique, for both counter-rotating and co-rotating cylinders. The curves were then empirically fit, yielding explicit analytic formulas for the critical Reynolds number for any radius ratio ($\eta$) and rotation ratio ($\mu$). For counter-rotating flows, the primary critical Reynolds number is determined by a single variable: the ratio of the nodal gap fraction to a known function of the radius ratio. The existence and influence of a nodal surface is shown experimentally for $\mu \cong -1.7$. For co-rotating flows, the important scaled variable was found to be the radius ratio divided by the nodal radius ratio. Comparisons of the resulting explicit stability formulas were made to existing analytic stability expressions and experimental data. Excellent quantitative agreement was found with data across the entire parameter space.

DOI: 10.1103/PhysRevE.75.047301 PACS number(s): 47.20.Qr, 47.80.Jk, 47.54.−r

## I. INTRODUCTION

The formation of the primary instability from unidirectional flow between concentric, rotating cylinders, Taylor-Couette (TC) flow, has been the subject of extensive study. In the seminal work by Taylor [1], linear stability theory (LST) was used to closely map the stability boundary as a function of rotation ratio, $\mu = \Omega_o/\Omega_i$, where $\Omega$ is the angular velocity and the subscripts "*o*" and "*i*" refer to the outer and inner cylinders, respectively. Extensive work has been done to expand upon LST, by solving LST for various radius ratios, $\eta = R_i/R_o$, [2–4], where $R$ is the radius, and extending it to approximate or asymptotic cases of rotation or radius ratio to develop analytic expressions for the stability boundary [4–6].

More recently, several authors have made important strides toward a complete, analytic functional form for the critical condition for the entire parameter space involving the rotation and radius ratios [7–9]. Coles [8] extended an analysis of Taylor's problem to non-narrow gaps by using a modified mean angular velocity, defined as an integral mean over the inviscidly unstable part of the gap. He also showed that the effect of geometry could be eliminated by proper choice of variables. However, the resultant implicit formulas err slightly as $\mu$ approaches zero and much more broadly at wide gaps.

Further advances were made by Esser and Grossmann [9], who derived analytic expressions for the stability boundary for all ranges of $\mu$ and $\eta$. Their analysis was based on a generalized Rayleigh criterion that included viscosity, a function that accounted for the boundary condition varying smoothly from a solid to a free surface as counter-rotation increased and the nodal surface becomes the important length scale, and an optimization of the location of the initial instability. This advance resulted in an implicit formula for the critical Reynolds number based on the inner cylinder, $\mathrm{Re}_c = (\Omega_i R_i d/\nu)_c$, in terms of a Reynolds number based on the outer cylinder, $\mathrm{Re}_o = \Omega_o R_o d/\nu$, and $\eta$, i.e., $\mathrm{Re}_c(\mathrm{Re}_o, \eta)$, that fits experimental data well at narrower radius ratios and extremely well for co-rotating flows. Here, $d$ is the gap, $R_o - R_i$, and $\nu$ is the kinematic viscosity. However, the accuracy of the function decays at wide gaps and in strongly counter-rotating flows. A better fit was found only after introducing the position of the disturbance as an additional fitting parameter.

The goal of the present work is to add to the above contributions by showing that the nature of the stability boundary, with respect to a characteristic governing length scale variable, is similar at all radius ratios. We then determine simple, explicit formulas for $\mathrm{Re}_c(\mu, \eta)$ by exploiting this self-similar functional dependence and analyzing experimental data for the entirety of the $(\mu, \eta)$ parameter space. The resulting explicit analytic expressions for the critical condition provide excellent quantitative agreement with experimental data.

The definition of parameters, derivation of the appropriate length scales, and the exploitation of the self-similarity of the stability boundary are described in Secs. II and III. These

TABLE I. References for experimental data of various radius and aspect ratios used in the analysis.

| Authors [reference] | $\eta$ | $\Gamma$ |
|---|---|---|
| Snyder, H.A [11], cf. 9 | 0.2, 0.5, 0.964 | >20[a] |
| Donnelly, R.J. *et al.* [12] | 0.5 | 30 |
| Andereck, *et al.* [13] | 0.883 | 20–48[b] |
| Dutcher, C. S. *et al.* [15] | 0.912 | 60.7 |
| Taylor, G.I. [1] | 0.9417 | 383 |

[a]For the smallest radius ratio, larger for higher radius ratios.
[b]Primarily with 30.

*Corresponding author. Electronic address: muller2@socrates.berkeley.edu

 

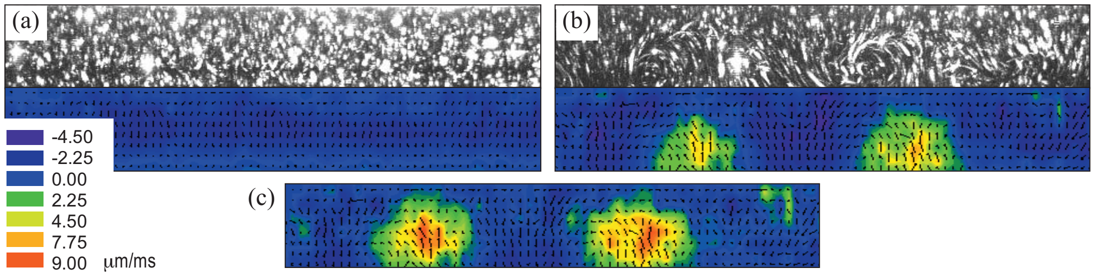


FIG. 1. (Color) Streaked images (top) and DPIV in the $(r,z)$ plane of TC geometry of $\eta=0.912$, $\Gamma=60.7$. The quiver plots represent the velocity field and the contour the radial velocity. (a) $\mathrm{Re_o}=-625$, $\mathrm{Re_c}=348$, $\mathrm{Re_i}=0.96\ \mathrm{Re_c}$, $\Theta=0.327$, (b) $\mathrm{Re_o}=-625$, $\mathrm{Re_c}=348$, $\mathrm{Re_i}=1.06\ \mathrm{Re_c}$.(c) Disturbance flow at $\mathrm{Re_o}=-625$, $\mathrm{Re_c}=348$, $\mathrm{Re_i}=1.06\ \mathrm{Re_c}$.

sections also include comparisons to experimental data (Table I) for various radius ratios and aspect ratios $\Gamma$ (where $\Gamma$=height/gap), and to an existing analytic expression for $\mathrm{Re_c}$.

## II. EXPLICIT ANALYTIC EXPRESSION, $\mu<0$

In counter-rotating flows ($\mu<0$), it is well known that there exists a line of zero angular velocity in the base azimuthal flow at a radial position $R_\mathrm{N}$, where $R_\mathrm{i}<R_\mathrm{N}<R_\mathrm{o}$. Therefore the Taylor-Couette (TC) geometry can be approximately thought of as two co-rotating TC geometries, one with a stationary outer free boundary at the nodal radius $R_\mathrm{N}$ and the other with a stationary inner free boundary at $R_\mathrm{N}$ [14]. The outer TC geometry is unconditionally stable, so the governing length scale for instability in the "inner" TC geometry is a function of the nodal radius length. This nodal radius is defined by the unidirectional angular velocity field parameters, and is a function of both radius and rotation ratios. However, the critical condition cannot be merely defined by the new radius ratio, $\eta_\mathrm{N}=R_\mathrm{i}/R_\mathrm{N}$, because the vortices formed marginally above the stability threshold are not confined to the nodal gap. This idea has been introduced by Esser and Grossmann [9], who described the nodal surface as a soft boundary, influenced by viscosity. Both the nodal surface and vortices that extend beyond the nodal gap are demonstrated experimentally in Fig. 1. The flow states seen in the figures were achieved by slowing increasing $\mathrm{Re_i}$ while holding the outer cylinder Reynolds number $\mathrm{Re_o}$ constant with $\eta=0.912$. The flow visualization images of the $(r,z)$ plane have been streaked over 330 ms to show $\mathbf{v}(r,z,t)$. The digital particle image velocimetry (DPIV) images have been averaged over 1000 ms, and they demonstrate the magnitude and direction of the velocity field. Figure 1 shows the gap just below and just above the instability for $\mathrm{Re_o}=-625$ in (a) and (b). The flow visualization is done in a plane of finite thickness with $d\theta$ approximately equal to 1.6° and as a result, in (a) the nodal surface is visible from the purely azimuthal velocity projected into this narrow slice of the $r$-$z$ plane. Via a similar projection, the disturbance flow is found in (c) by subtracting off any contribution from the azimuthal flow in (a).

Figure 1 suggests that the appropriate dimensionless length scale for counter-rotating TC flows is the nodal gap to original gap ratio, $\Theta=(R_\mathrm{N}-R_\mathrm{i})/(R_\mathrm{o}-R_\mathrm{i})$. By solving for $R_\mathrm{N}$ using the known unidirectional solution for the azimuthal angular velocity field, the counter-rotation dimensionless length scale is shown to be $\Theta=(\eta)(1-1/\eta_\mathrm{N})/(\eta-1)$, where $\eta_\mathrm{N}=[(\eta^2-\mu)/(1-\mu)]^{1/2}$. Profiles of the critical Reynolds number $\mathrm{Re_c}$, scaled with $\mathrm{Re_c}$ for the limiting case of stationary outer cylinder $\mathrm{Re_c}(\mu=0)$, appear self-similar for all radius ratios $\eta$ when plotted as a function of $\Theta$. As a result, the data can be collapsed onto a single curve by scaling the dimensionless length scale $\Theta$ by a function of radius ratio $f(\eta)$, found empirically in Fig. 2.

The pseudoempirical explicit formula [Eq. (1)] fits the available data for the existing range of radius ratios ($0.2<\eta<0.964$) and rotation ratios for counter-rotation ($-7.17<\mu<0$), and is given by

$$\mathrm{Re}_c(\eta,\mu<0)/\mathrm{Re}_c(\eta,\mu=0) = 1+0.025\,724\left(\frac{\exp\{4.772[1-\Theta/f(\eta)]\}}{\Theta/f(\eta)}-1\right), \quad (1)$$

$$\mathrm{Re}_c(\eta,\mu=0) = 10.812\,94/\eta + 41.450\,25/(1-\eta)^{1/2} - 11.675\,78, \quad (2)$$

$$f(\eta) = 1.03 - \exp[-(3.584)\eta]. \quad (3)$$

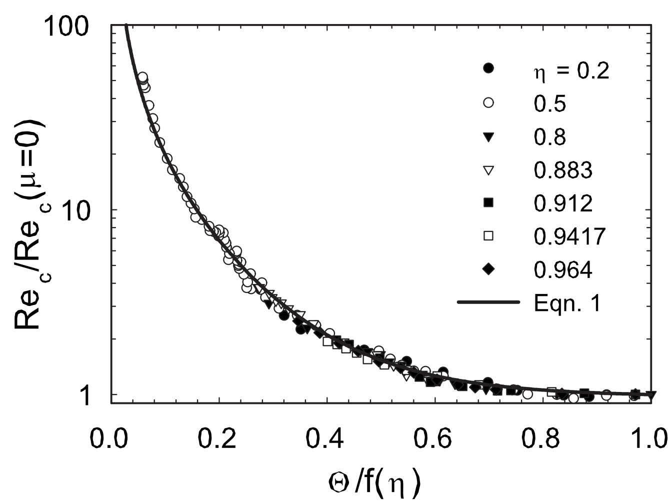


FIG. 2. Collapse of counter-rotating TC data for an expansive range of $\mu$, $\eta$.

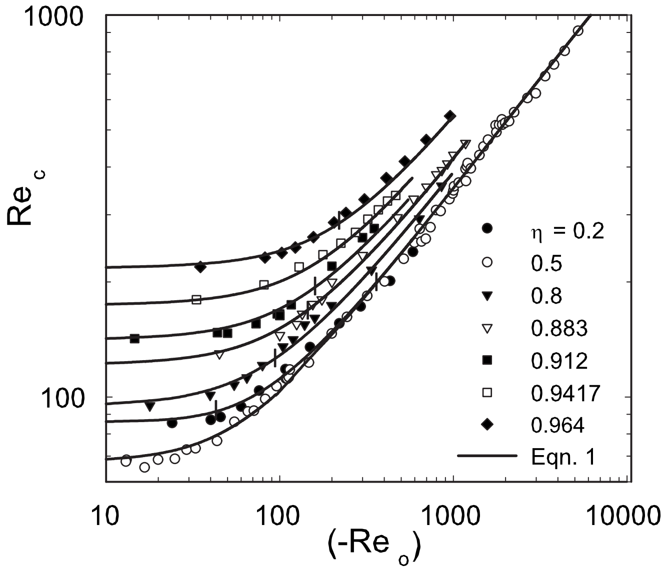


FIG. 3. Comparison of counter-rotating TC data to semiempirical formula [Eqs. (1)–(3)] for an expansive range of $\mu, \eta$. Data points to the (left/ right) of the vertical dashes represent primary transitions to the (Taylor vortex flow/spiral vortex flow) regime. For $\eta$=0.9417, flow type was not indicated on the marginal stability curve.

Figure 3 shows the same data on the primary instability, replotted on the standard $\mathrm{Re_i}(\mathrm{Re_o})$ coordinates, along with Eq. (1), for various $\eta$, and confirms that the empirical scaling discussed above does an excellent job of fitting all the data over the existing many orders of magnitude.

### III. EXPLICIT ANALYTIC EXPRESSION, $\mu > 0$

In the absence of counter-rotation, the dominant length scale is no longer related to the nodal line of counter-rotation, and $\mathrm{Re_c}$, as defined above, is no longer the best representation of the driving force for destabilization of the flow. Instead, the rotation number, $R_\Omega = (1-\eta)(1+\mu/\eta)/(\mu-1)$, defined by Dubrulle *et al.* [10], captures the relevant dynamic driving force in rotating shear flows in the absence of a nodal surface, which we now take as our dependent variable. In order to display the data in a plane that is characterized by self-similarity, a normalized rotation number, $[R_\Omega - R_\Omega(\mu=0)]/R_\Omega(\mu=0)$ is used, where $R_\Omega(\mu=0) = -(1-\eta)$ is the critical condition at the stationary outer cylinder limit. The independent variable, $\mathrm{Re_c}$, also scaled by the stationary outer cylinder critical condition, is transposed by unity to produce a zero intercept, resulting in $[\mathrm{Re_c} - \mathrm{Re_c}(\mu=0)]/\mathrm{Re_c}(\mu=0)$. When the rotation number is scaled as defined above by the asymptotic values at large inner cylinder rotation, $(1-\eta)/\eta$, the resultant curves are similar and given by

$$\frac{R_\Omega - R_\Omega(\mu=0)}{R_\Omega(\mu=0)} = \frac{\eta}{1-\eta} \times \left[1 - \exp\left(-\frac{\{[\mathrm{Re}_c - \mathrm{Re}_c(\mu=0)]/\mathrm{Re}_c(\mu=0)\}^{\lambda_1(\eta)}}{\lambda_2(\eta)}\right)\right] \tag{4}$$

$$\lambda_1(\eta) = 0.587\,225 + 0.013\,253/(1-\eta), \tag{5}$$

$$\lambda_2(\eta) = 0.604\,419 + 0.069\,421/(1-\eta). \tag{6}$$

The margins of stability for various radius ratios can be collapsed onto one curve in this plane using the invertible double exponential form of Eq. (4) with two modes, $\lambda_1$ and $\lambda_2$, capturing the dynamics at small and large $\mathrm{Re_i}$, respectively. Inversion of Eq. (4) provides an analytic expression for the critical $\mathrm{Re_i}$ as a function of both $\eta$ and $\mu$ and is given in Eq. (7),

$$\mathrm{Re}_c(\eta,\mu>0)/\mathrm{Re}_c(\eta,\mu=0) = 1 + [\lambda_2(\eta)\ln(\Psi(\eta,\mu))]^{1/\lambda_1(\eta)}, \tag{7}$$

$$\Psi = \frac{1-\mu}{1-\mu/\eta^2} = \left(\frac{\eta}{\eta_N}\right)^2. \tag{8}$$

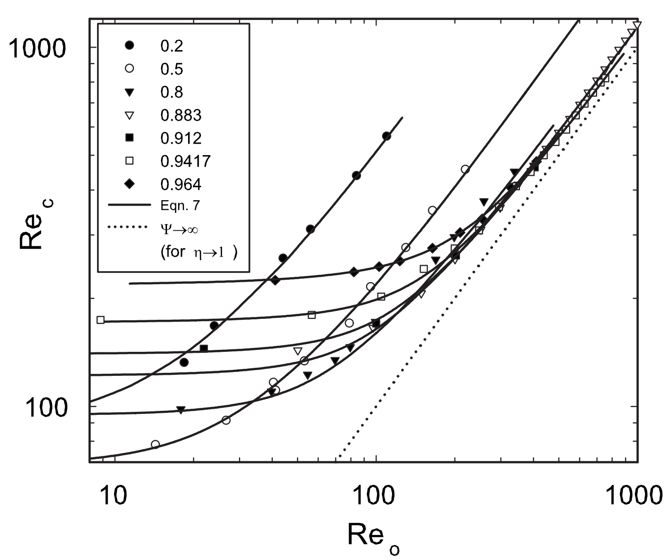


FIG. 4. Comparison of co-rotating TC data to Eq. (7).

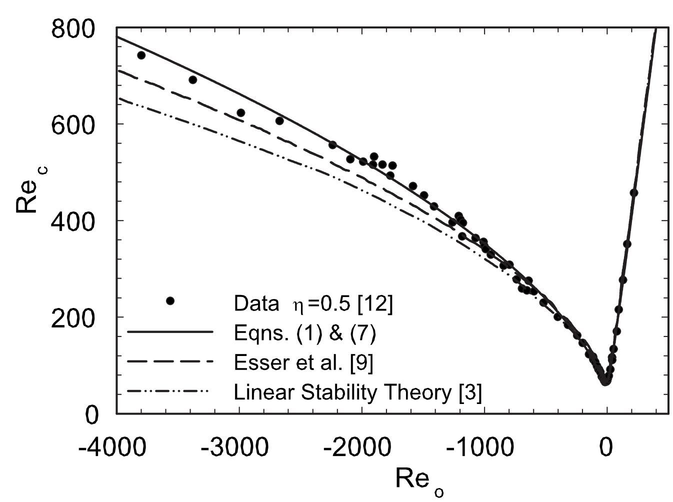


FIG. 5. Comparison of calculated values of $\mathrm{Re_c}(\mathrm{Re_o}, \eta=0.5)$.

$\Psi$ represents an effective dimensionless dominant length scale for the co-rotation regime. This length scale is the ratio of the co-rotation inertia stability parameter $(\Omega_o - \Omega_i)/\Omega_i$ to the Rayleigh inviscid fluid stability parameter and represents a coordinate transformation over the accessible range of co-rotation data. As a result, $\Psi = 1$ corresponds to flows with a stationary outer cylinder and as $\Psi$ approaches infinity Eq. (7) approaches the corresponding inviscid stability limit [shown for the narrow gap limit by the dashed line in Fig. (4)]. Figure 4 shows the experimental data are well described by Eq. (7) over the existing orders of magnitude of $\mathrm{Re}_i$ and $\mathrm{Re}_o$.

Figure 5 shows a representative comparison of the analytic expressions for $\mathrm{Re}_c$ given in Eqs. (1) and (7) to both that of Esser and Grossman [9] and linear stability theory [3], demonstrating that this work's phenomenologically scaled empirical expressions best capture the data for $\eta = 0.5$. The present proposed analytic formulas were compared to those of Esser and Grossman [9] for experimental data representing a wide range of $\mu$ and $\eta$. In nearly all cases the present work shows closer agreement with the experiments; the percentage errors with the current formulas are typically two to four times smaller than with the equations in Ref. [9].

## IV. SUMMARY

For a given rotation ratio and radius ratio, the critical Reynolds number based on the inner cylinder, $\mathrm{Re}_c(\eta, \mu)$, for the formation of the primary TC instability can be explicitly found from the simple analytic formulas presented in this paper. Remembering that $\mu = \eta \mathrm{Re}_o / \mathrm{Re}_i$, then $\mathrm{Re}_c(\eta, \mathrm{Re}_o)$ can be found by solving the expressions numerically. This paper has also shown that the important dimensionless length scales, $\Psi(\eta, \mu)$ and $\Theta(\eta, \mu)$, can be used to fully describe the dependence of the critical conditions on radius ratio. To the best of our knowledge, these simple explicit formulas derived from phenomenological scaling of experimental data provide the best quantitative agreement over the complete range of $\mu$ and $\eta$ of any analytic expression for the primary stability boundary for TC flows.

## ACKNOWLEDGMENT

The authors are grateful for the support of the National Science Foundation through Grant No. CTS-0335169. C.S.D. acknowledges support from the National Science Foundation Graduate Research Program.

[1] G. I. Taylor, Philos. Trans. R. Soc. London, Ser. A **223**, 289 (1923).
[2] E. M. Sparrow, W. D. Munro, and V. K. Jonsson, J. Fluid Mech. **20**, 1 (1964).
[3] R. Gebhardt and S. Grossmann, Z. Phys. B: Condens. Matter **90**, 475 (1993).
[4] S. Chandrasekhar, *Hydrodynamic and Hydromagnetic Stability*, 1st Ed. (Clarendon Press, Oxford, 1961).
[5] D. D. Joseph, *Stability of Fluid Motions I*, 1st Ed. (Springer-Verlag, Berlin, 1976).
[6] P. G. Drazin and W. H. Reid, *Hydrodynamic Stability*, 1st Ed. (Cambridge University Press, Cambridge, England, 1981).
[7] J. Walowit, S. Tsao, and R. C. DiPrima, J. Appl. Mech. **31**, 585 (1964).
[8] D. Coles, J. Appl. Mech. **34**, 529 (1967).
[9] A. Esser and S. Grossmann, Phys. Fluids **8**, 1814 (1996).
[10] B. Dubrulle *et al.*, Phys. Fluids **17**, 095103 (2005).
[11] H. A. Snyder, Phys. Fluids **11**, 8 (1968).
[12] R. J. Donnelly and D. Futlz, Proc. R. Soc. London, Ser. A **258**, 1292 (1960).
[13] C. D. Andereck, S. S. Liu, and H. L. Swinney, J. Fluid Mech. **164**, 155 (1986).
[14] B. Echhardt and D. Yao, Chaos, Solitons Fractals **5**, 2073 (1995).
[15] C. S. Dutcher and S. J. Muller (unpublished).